Pergamon

0306-4549(95)00017-8

Ann. Nucl. Energy Vol. 23, No. 3, pp. 217–228, 1996

0306-4549/96 $15.00 + 0.00

VELOCITY PROFILE EFFECTS ON NEUTRON CROSS-SPECTRA IN BWRs

M. ANTONOPOULOS-DOMIS and S. KADI

Department of Electrical and Computer Engineering, Aristotle University of Thessaloniki, 540 06 Thessaloniki, Greece

(Received 14 February 1995)

Abstract The effects of velocity profiles of void propagation are investigated with a 2-D, two neutron group model. The model is solved numerically. It is shown that the double slope of phase observed in some measurements may be the effect of such a profile. The mechanisms of this effect are investigated.

1. INTRODUCTION

The fact that a disturbance propagating upwards with constant velocity in a reactor core will produce a linear dependence on frequency, of the phase of the cross-spectra of neutron detectors placed along different heights on the same vertical line, has been used to determine void propagation velocities in BWRs and has been the subject of extensive theoretical and experimental investigations (Stekelenburg and Van der Hagen, 1993). Some experimental measurements presented two linear slopes of the phase at the upper part of the core: one at low frequencies and a different one at higher frequencies (Kosaly *et al.*, 1977; Behringer and Crowe, 1981; Federico *et al.*, 1982; Kleiss *et al.*, 1985). Several possible interpretations of this phenomenon have been suggested, namely that the detectors may see different velocities at surrounding subassemblies, that there may be boiling in the bypass region where detectors are placed, etc. (Kosaly, 1980). It has been suggested (Behringer, 1983; Luebbesmeyer, 1983; Kleiss *et al.*, 1985) that this may be due to velocity profile effects. Luebbesmeyer (1983) demonstrated this using synthetic signals. In the present work we investigate the effects on neutron spectra of disturbances propagating upwards in a reactor core, not with uniform velocity, but with a velocity profile. To this aim a two-dimensional, two neutron energy group model is used and solved numerically in the frequency domain. The simulation model and its solution is described in Section 2. Results and discussion are presented in Section 3. We end with the conclusions in Section 4.

2. THE MODEL

A two-dimensional, two neutron group, bare homogeneous reactor model is used. The model equations read

$$\begin{aligned}
\frac{1}{v_1}\frac{\partial \Phi_1(r,t)}{\partial t} &= D_1\nabla^2\Phi_1(r,t) - \Sigma_R\Phi_1(r,t) + (1-\beta)\nu\Sigma_f\Phi_2(r,t) + \lambda C(r,t)\\
\frac{1}{v_2}\frac{\partial \Phi_2(r,t)}{\partial t} &= D_1\nabla^2\Phi_2(r,t) - \Sigma_{a2}\Phi_2(r,t) + \nu\Sigma_{12}\Phi_1(r,t)\\
\frac{\partial C(r,t)}{\partial t} &= \beta\nu\Sigma_f\Phi_2(r,t) - \lambda C(r,t)
\end{aligned} \tag{1}$$

where the symbols have their usual meaning. We assume that the system is critical and that neutron density

fluctuations are excited by fluctuations $\delta\Sigma_{a2}(\underline{r}, t)$ of the thermal absorption cross-section $\Sigma_{a2}(\underline{r}, t)$. Splitting fast Φ_1 and thermal Φ_2 fluxes and delayed neutron precursor density into static and fluctuating parts, i.e.

$$\Phi_i(\underline{r}, t) = \Phi_{i0}(\underline{r}) + \delta\Phi_i(\underline{r}, t) \qquad i = 1, 2$$
$$C(\underline{r}, t) = C_0(\underline{r}) + \delta C(\underline{r}, t) \tag{2}$$

where $\underline{r}$ is space and t time variables, using the static equations, linearizing and Fourier transforming, the model equations read

$$\nabla^2\delta\hat{\Phi}_1(\underline{r}, \omega) - k_1^2\delta\hat{\Phi}_1(\underline{r}, \omega) + b_1\delta\hat{\Phi}_2(\underline{r}, \omega) = 0$$
$$\nabla^2\delta\hat{\Phi}_2(\underline{r}, \omega) - k_2^2\delta\hat{\Phi}_2(\underline{r}, \omega) + b_2\delta\hat{\Phi}_1(\underline{r}, \omega) = S(\underline{r}, \omega)$$
$$\hat{S}(\underline{r}, \omega) = \frac{\Sigma_{a20}}{D_2}\Phi_{20}(r)\frac{\delta\hat{\Sigma}_{a2}(r, \omega)}{\Sigma_{a20}} \tag{3}$$

where $\hat{f}(\omega)$ is Fourier Transform of $f(t)$ and,

$$k_1^2 = \frac{1}{D_1}\left(\Sigma_R + \frac{j\omega}{v_1}\right), \qquad b_1 = \frac{\nu\Sigma_f}{D_1}\left(1 - \frac{j\beta\omega}{\lambda + j\omega}\right)$$
$$k_2^2 = \frac{1}{D_2}\left(\Sigma_{a20} + \frac{j\omega}{v_2}\right), \qquad b_2 = \frac{\Sigma_{12}}{D_2} \tag{4}$$

The bare core is two-dimensional extending in the x (radial) and z (axial) directions. The model equations are solved numerically, with finite difference approximations to derivatives, on a grid of $x_n = n\cdot\Delta x$, $z_m = m\cdot\Delta z$ computational points. Bubble propagation velocity profiles are simulated by setting the excitation term $\delta\hat{\Sigma}_{a2}(\underline{r}, \omega)/\Sigma_{a20}$ as follows.

$$\frac{\delta\hat{\Sigma}_{a2}}{\Sigma_{a20}} = -\sum_{n=k}^{n=k+p}\delta\hat{\alpha}_{n0}(\omega)\cdot\exp\left(-j\omega\frac{z_n}{V_n}\right)\delta(x - x_n) \tag{5}$$

It can be seen from equation (5) that a discrete velocity profile is imposed on $(p + 1)$ adjacent lines of the computation grid. At each such line x_n the velocity V_n of bubble propagation is constant along the height of the core, but different from the propagation velocity in the other p computation lines. Such a group of $(p + 1)$ line-disturbances we will call "a velocity profile" or "a channel". Results are presented here for $p = 8$, i.e. for a discrete profile of nine lines. We call peaking factor the ratio of maximum to minimum velocity. For $p = 0$ we have a single line excitation. The Fourier Transform $\delta\hat{\alpha}_{n0}(\omega)$ of void fraction fluctuation at the channel inlet is assumed to be,

$$\delta\hat{\alpha}_{n0}(\omega) = 1 \tag{6}$$

i.e. white noise of the same power for all $(p + 1)$ lines. It should be noted that by setting the excitation as in equation (5), computing the neutron response $\delta\hat{\Phi}_2(\underline{r}, \omega)$ and from this computing the spectra, it is implicitly assumed that the void fraction fluctuations $\delta\hat{\alpha}_{n0}(\omega)$ are correlated.

Verification of the code was done by simulation of a 1-dimensional model with the 2-dimensional code (Antonopoulos-Domis *et al.*, 1995).

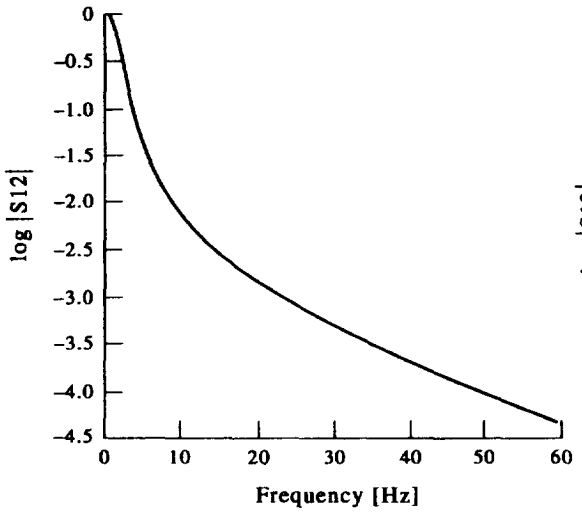

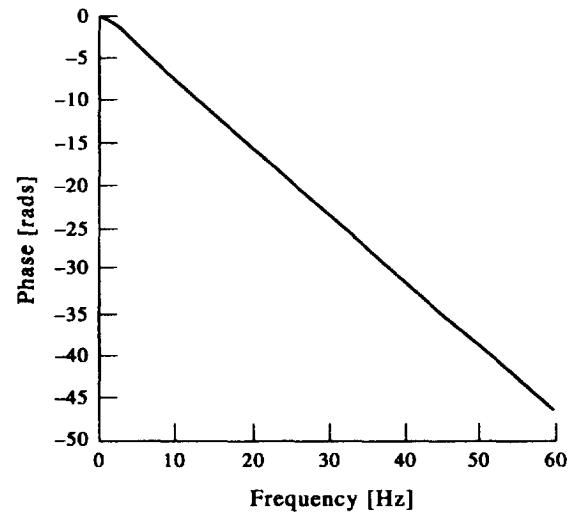

Fig. 1. Neutron cross-spectrum S_{12} between $z_2 = 306$ cm and $z_1 = 216$ cm, for a single-line excitation with $V = 720$ cm/s.

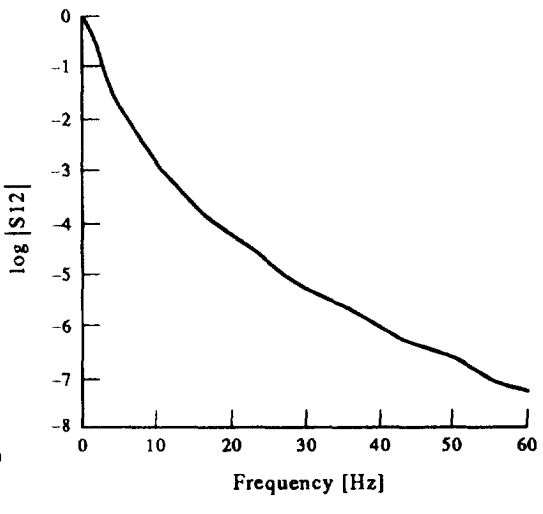

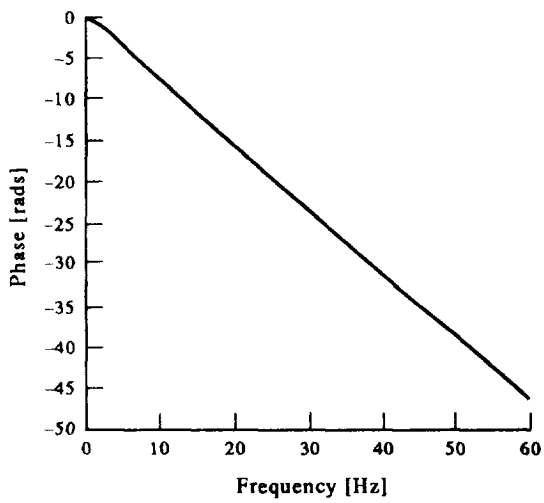

Fig. 2. Neutron cross-spectrum S_{12} between $z_2 = 306$ cm and $z_1 = 216$ cm, for a flat velocity profile. Propagation velocity $V = 720$ cm/s.

3. RESULTS AND DISCUSSION

All results presented here were obtained for a homogeneous, critical bare core of width 200 cm and height 360 cm. Neutron cross-spectra are computed and presented here, between positions z_1 and z_2 at the same radial position x, at a distance

$$\Delta x = 3.33 \text{ cm} \cong L_2 \equiv \sqrt{D_2/\Sigma_{a2}}$$

from the edge line of the profile.

Figure 1 presents the cross-spectrum of neutron fluctuations excited by a single line excitation. It can be seen that, for the specific core-size, the modulus is a smooth function of frequency and the phase is a linear function of frequency, the slope of which corresponds exactly to the propagation velocity of 720 cm/s of the excitation. For significantly smaller cores, for which reactivity effects are of comparable magnitude to

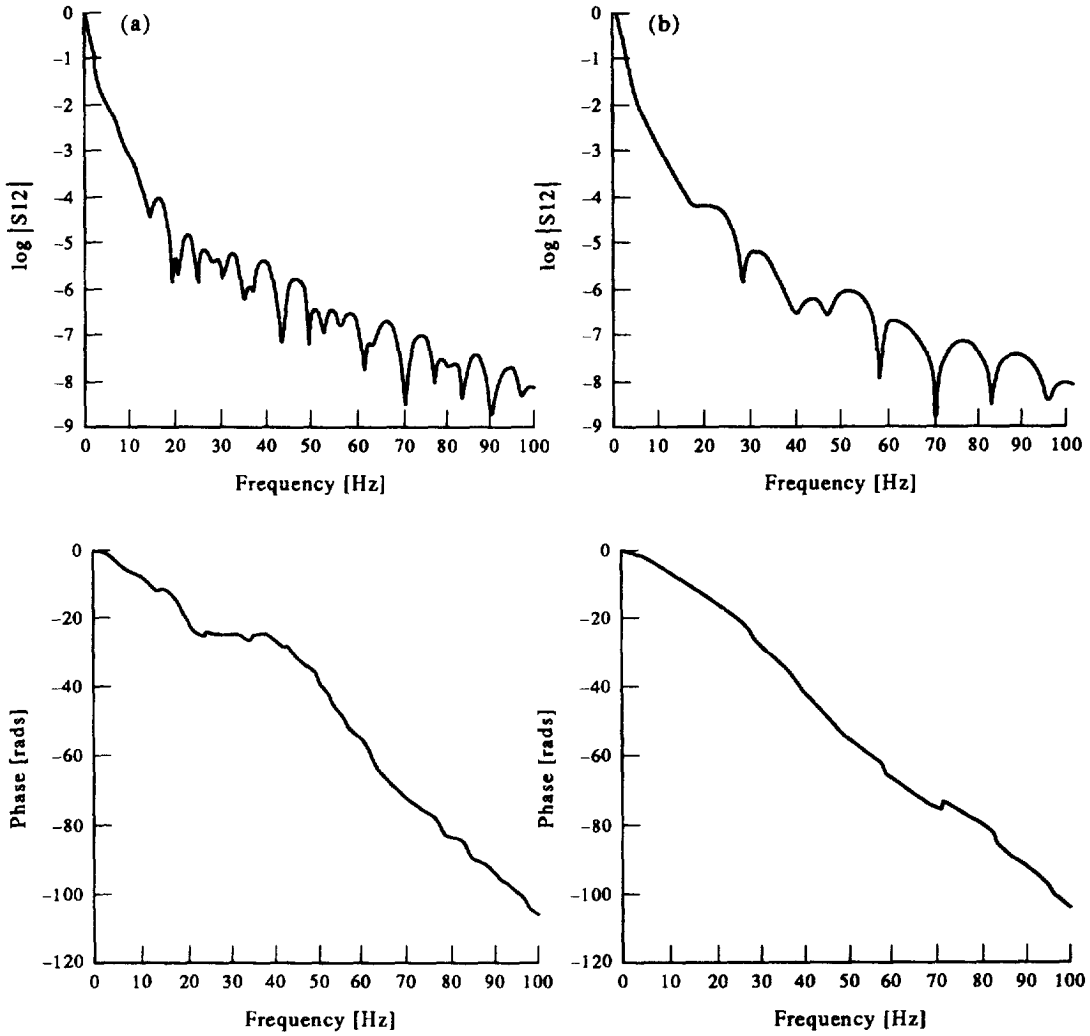

Fig. 3. Neutron cross-spectra S_{12} between (a) *z2 = 306 cm and* $z_1 = 216$ cm, i.e. at the upper part of the core, and (b) $z_2 = 162$ cm and $z_1 = 72$ cm, i.e. at the lower part of the core. Turbulent-like velocity profile with $V_{max} = 720$ cm/s and $V_{min} = 504$ cm/s.

attenuation (local) effects, the magnitude presents deeps and peaks and the phase presents undulations around a line corresponding again to the propagation velocity.

Figure 2 presents the cross-spectrum of neutron fluctuations excited by a flat velocity profile, i.e. by using $V_n = V = 720$ cm/s, $n = k$ to $n = k + 8$ in equation (5). It can be seen that the phase is a linear function of frequency corresponding to $V = 720$ cm/s. The magnitude is almost a smooth function of frequency with very weak undulations.

Figure 3 presents cross-spectra of neutron response due to a "turbulent-like" velocity profile with maximum velocity, at channel center-line, of $V_{max} = 720$ cm/s and minimum velocity, at channel edge-lines, of $V_{min} = 504$ cm/s, i.e. a peaking factor of 1.428. It can be seen that the modulus of the cross-spectra presents clear deeps and peaks. At the upper part of the core [Fig. 3(a)] the deeps start at lower frequencies than at the lower part of the core [Fig. 3(b)]. At the lower part of the core the phase can be interpreted as presenting two slopes. Fitting a straight line at low frequencies, i.e. between 0 and 28 Hz, a velocity of $V_{low} = 693$ cm/s, i.e. close to $V_{max} = 720$ cm/s, is inferred. Fitting a straight line at high frequencies, i.e. from 30 to 100 Hz, a

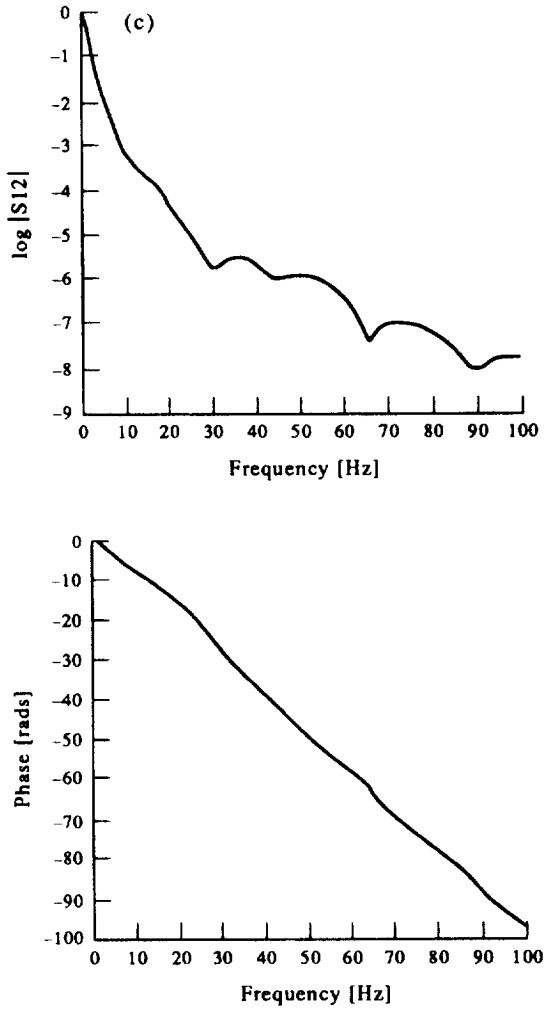

Fig. 3. (c) Neutron cross-spectra S_{12} between $z_2 = 162$ *cm and* $z_1 = 72$ cm, i.e. at the lower part of the core. Turbulent-like velocity profile with $V_{max} = 720$ cm/s and $V_{min} = 576$ cm/s.

velocity of $V_{high} = 537$ cm/s is inferred, i.e. close to the edge velocity $V_{min} = 504$ cm/s. At the upper part of the core phase undulations are more pronounced and start at lower frequencies. Fitting a straight line at low frequencies, i.e. from 0 to 20 Hz, a velocity of $V_{low} = 718$ cm/s is inferred, which is practically equal to $V_{max} = 720$ cm/s. Fitting a straight line at high frequencies, for example from 50 to 100 Hz, a velocity $V_{high} = 437$ cm/s is inferred. This is clearly smaller than the minimum velocity $V_{min} = 504$ cm/s of the profile.

One could understand velocities inferred from the slope of the phase to have values between V_{min} and V_{max} as a result of the summation of the individual responses to each line excitation of the profile. However, it is impossible for such a summation to yield a velocity smaller than V_{min}. A possible explanation is that what is interpreted as a second slope at high frequencies may in fact be a long undulation.

Figure 3(c) presents a neutron cross-spectrum, in the case of a turbulent-like velocity profile with a peaking factor of 1.25, i.e. smaller than the previous one. It can be seen that we have similar, but less pronounced, phenomena. In general the higher the peaking factor the more pronounced are the observed effects. The model runs show that profile effects are much stronger in the upper part of the core than in the lower part. These two observations hold irrespective of the form of the profile, i.e. for turbulent, laminar and other profiles.

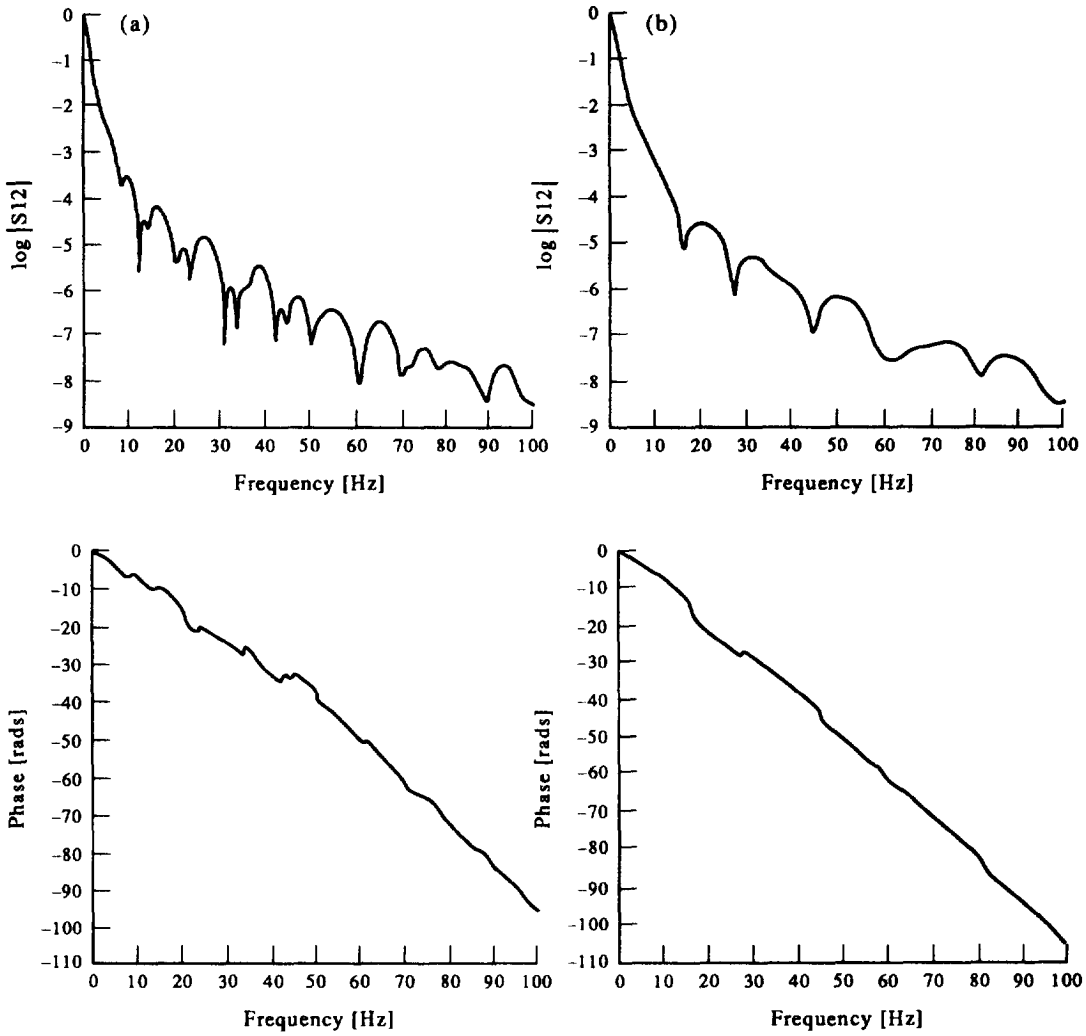

Fig. 4. Neutron cross-spectra S_{12} between (a) $z_2 = 306$ cm and $z_1 = 216$ cm, i.e. at the upper part of the core, and (b) $z_2 = 162$ cm and $z_1 = 72$ cm, i.e. at the lower part of the core. Laminar-like velocity profile with $V_{max} = 720$ cm/s and $V_{min} = 504$ cm/s.

Figure 4 presents cross-spectra of neutron response due to a "laminar-like" velocity profile. At the lower part of the core the phase appears to have a single slope with small undulations around it. The velocity inferred from this slope is 547 cm/s, i.e. in between V_{max} and V_{min}. At the upper part of the core two slopes appear. Fitting a straight line at low frequencies (0–50 Hz) a velocity $V_{low} = 692$ cm/s, i.e. close to V_{max}, is inferred. The velocity inferred from the high frequency range of the phase is practically equal to the edge velocity V_{min}.

Exciting the model with different velocity profiles, more than one slope in the phase of neutron cross-spectra is observed. The present numerical experiments clearly demonstrate that the double slope observed in some experimental measurements can be attributed to the effect of a velocity profile of void propagation.

It is of obvious interest to understand the mechanism(s) through which a velocity profile produces more than one slope in the phase of neutron cross-spectra. In the actual case of BWRs the neutron detectors, being in the bypass region, are closer to the edges of the fuel subassemblies, thus closer to the lower velocities and further away from the higher velocities, if void propagation velocity profiles resemble turbulent or

laminar profiles. This is simulated by the model runs reported here (Figs 3 and 4). It should, however, be mentioned that in the simulation results more than one slope may be observed in the phase of neutron cross-spectra, irrespective of the velocity profile, provided this is not a flat one.

Let us restrict the discussion to the model. Let $\delta\hat{\Phi}_n(x, z, \omega)$ be the response at (x, z) due to the line excitation at x_n,

$$\delta\hat{\Phi}_n(x, z, \omega) = \delta\hat{\alpha}_{n0}|A_n(x, z, \omega)|e^{j\varphi_n(x,z,\omega)} \tag{7}$$

where $\delta\hat{\alpha}_{n0}\cdot|A_n|$ is the amplitude and φ_n the phase of the transfer function between $\delta\hat{\Phi}_n$ and $\delta\hat{\alpha}_{n0}$ the void fraction at the core inlet. Clearly, the total response $\delta\hat{\Phi}(x, z, \omega)$ due to all line excitations is the sum of the responses to the individual excitations.

$$\delta\hat{\Phi}(x, z, \omega) = \sum_n \delta\hat{\alpha}_{n0}|A_n|e^{j\varphi_n} \tag{8}$$

The phase of $\delta\hat{\Phi}(x, z, \omega)$ depends on both the amplitude $|A_n|$ and the phase φ_n of the response to each individual excitation. The amplitude $|A_n|$ depends on the distance $|\Delta x| = |x - x_n|$ from the line excitation position x_n and on the relaxation length which, in general, is frequency dependent.

To simplify matters let us consider not a velocity profile but only two line excitations, one at x_1 propagating upwards with velocity V_1 and another one at x_2 with velocity V_2. Let the response at (x, z) due to the first one be $\delta\hat{\Phi}_1(x, z, \omega)$ and due to the second one $\delta\hat{\Phi}_2(x, z, \omega)$. The response $\delta\hat{\Phi}(x, z, \omega)$ due to both excitations is,

$$\begin{aligned}\delta\hat{\Phi}(x, z, \omega) &= \delta\hat{\Phi}_1(x, z, \omega) + \delta\hat{\Phi}_2(x, z, \omega)\\ &= \delta\hat{\alpha}_{10}|A_1(x, z, \omega)|e^{j\varphi_1(x,z,\omega)} + \delta\hat{\alpha}_{20}|A_2(x, z, \omega)|e^{j\varphi_2(x,z,\omega)}\end{aligned} \tag{9}$$

The neutron cross-spectrum S_{AB} between positions (x, z_A) and (x, z_B) is

$$\begin{aligned}S_{AB} &\equiv E\{\delta\hat{\Phi}(x, z_B, \omega)\delta\hat{\Phi}^*(x, z_A, \omega)\}\\ &= E\{|\delta\hat{\alpha}_{10}|^2\}|A_{1B}||A_{1A}|e^{j(\varphi_{1B} - \varphi_{1A})} + E\{|\delta\hat{\alpha}_{20}|^2\}|A_{2B}||A_{2A}|e^{j(\varphi_{2B} - \varphi_{2A})}\\ &\quad + E\{\delta\hat{\alpha}_{10}\delta\hat{\alpha}^*_{20}\}|A_{1B}||A_{2A}|e^{j(\varphi_{1B} - \varphi_{2A})} + E\{\delta\hat{\alpha}_{20}\delta\hat{\alpha}^*_{10}\}|A_{2B}||A_{1A}|e^{j(\varphi_{2B} - \varphi_{1A})}\end{aligned} \tag{10}$$

where * denotes complex conjugate, $E\{.\}$ denotes the expected value of $\{.\}$ and $|A_{ik}|e^{j\varphi_{ik}}$ denotes the response at (x, z_k) due to a line excitation at x_i, $i = 1, 2$ and $k = A, B$. If $\delta\alpha_{10}$ and $\delta\alpha_{20}$ are statistically independent the cross-terms [last two terms in equation (10)] disappear.

To eliminate attenuation differences let us first consider the cross-spectrum between (x, z_B) and (x, z_A) at equal distances $|x - x_1| = |x - x_2|$ from the line excitations at x_1 and x_2, i.e. between points at z_B and z_A on the middle line x between x_1 and x_2. In this case we may take

$$|A_{1A}| \cong |A_{2A}| \cong |A_{1B}| \cong |A_{2B}| \tag{11}$$

Let us further neglect global effects, i.e. assume that the phase of $\delta\Phi(x, z, \omega)$ is $\exp(-j\omega z/V)$ where V is the void velocity at x.

Then it can be readily shown analytically that, without the cross-terms of equation (10), the modulus of the cross-spectrum will have deeps at frequencies (Kozma, 1991).

$$f = \frac{2k + 1}{2(\tau_1 - \tau_2)} \qquad k = 0, 1, 2, \ldots \tag{12}$$

where $\tau_1 = \Delta z/V_1$, $\tau_2 = \Delta z/V_2$ and the phase of the cross-spectrum is $-\omega(\tau_1 + \tau_2)/2$, i.e. linear with frequency.

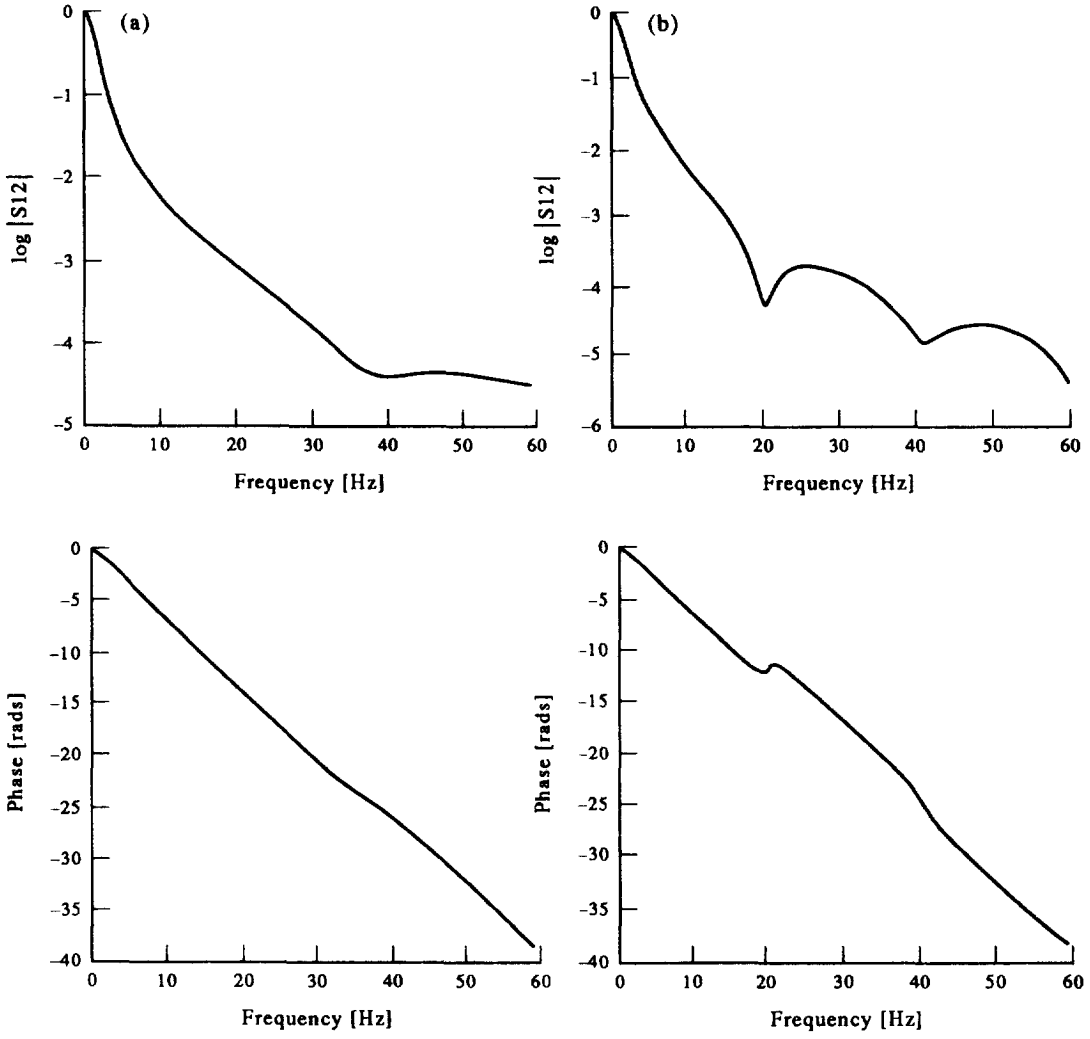

Fig. 5. Neutron cross-spectra S_{12} between $z_2 = 144$ cm and $z_1 = 70$ cm for two line excitations at equal distances from the detectors (a) without cross terms, (b) with cross terms.

Allowing the amplitudes in equation (11) to have small differences of the order of 10% it can be verified numerically that the phase will present long undulations around a straight line near the line $-\omega(\tau_1 + \tau_2)/2$.

Figure 5(a) presents the cross-spectrum obtained from the simulation code for $|x - x_1| = |x - x_2|$, assuming that $\delta\hat{\alpha}_{10}$ and $\delta\hat{\alpha}_{20}$ are statistically independent, i.e. without the cross-terms. Note that in this run of the simulation code global effects are included but are not significant. It can be seen that the magnitude presents a deep at 40 Hz, i.e. very near the first frequency predicted by equation (12), the small difference being due to the fact that equation (11) does not hold exactly. The phase presents a long undulation with a crossing at the same frequency, which experimentally would not necessarily be recognized as such. This phase could in an experiment be interpreted as a straight line. The transit time inferred from this line is near to $(\tau_1 + \tau_2)/2$, as expected in this case.

The void fraction at the different horizontal positions of the same subassembly should be expected to be correlated. Assuming that $\delta\hat{\alpha}_{10}$ and $\delta\hat{\alpha}_{20}$ are correlated, i.e. including cross-terms in equation (10), and that $|\delta\hat{\alpha}_{10}| = |\delta\hat{\alpha}_{20}| = 1$ and neglecting global effects, it can be shown analytically that the magnitude of the cross-

spectrum will have deeps at frequencies

$$f = \frac{2k+1}{2\left(\frac{z_A}{V_1} - \frac{z_A}{V_2}\right)} \quad \text{and} \quad f = \frac{2k+1}{2\left(\frac{z_B}{V_1} - \frac{z_B}{V_2}\right)} \qquad k = 0, 1, 2, \ldots \tag{13}$$

Note that for $V_1 = V_2$ the frequencies of equations (12) and (13) go to infinity, i.e. there are no deeps in the cross-spectra. Figure 5(b) presents the cross-spectrum obtained from the simulation code for $|x - x_1| = |x - x_2|$, including the cross-terms and assuming that $|\delta\hat{\alpha}_{10}| = |\delta\hat{\alpha}_{20}| = 1$. Note that in this run of the simulation code global effects are included but are not significant. The magnitude presents deeps very near the frequencies predicted by equation (13) and the phase long undulations with crossings of a straight line at the same frequencies. This straight line corresponds to a transit time near $(\tau_1 + \tau_2)/2$. We may note that at low frequencies the phase follows exactly this straight line. Note that the long undulations present at higher frequencies could be interpreted in an experiment as a second slope. The fact that this behavior depends on the actual positions z_B and z_A could be a possible explanation of the experimental observation that the second slope appears at the upper part of the core only. As mentioned already, in these findings attenuation effects do not play a role; these phenomena are simply the effect of the sum of the responses due to the two excitations propagating with different velocities.

In the actual case of BWRs where the neutron detectors are placed in the bypass region, the detectors are closer to the edge of the subassembly where velocities are small in comparison with velocities further away from the subassembly edge. Let us consider the 2-D model results for a similar case with two only line excitations. Figure 6(a) presents the neutron cross-spectrum in the case of two line excitations, one with velocity of $V_1 = 504$ cm/s at a distance $\Delta x = 3.33$ cm from the "detectors" and the other with velocity $V_2 = 720$ cm/s at a distance $\Delta x = 9.96$ cm from the "detectors". At high frequencies, say above 20 Hz, the phase decreases linearly with frequency, with a slope corresponding to a propagation velocity almost exactly equal to the small velocity of 504 cm/s (which is closer to the detectors than the larger velocity). Least squares fitting of a straight line at low frequencies, from 0 to 15 Hz, gives a slope corresponding to a velocity of about 662 cm/s, i.e. in between V_1 and V_2. Figure 6(b) presents the ratio $|A_1|/|A_2|$, where $|A_i|$ is the amplitude of the response due to the excitation propagating with velocity V_i. It can be seen that at high frequencies the amplitude $|A_1|$, of the response due to the excitation being closer to the detectors, is much larger than $|A_2|$; hence, in the sum of the two responses, the response due to $V_1 = 504$ cm/s predominates. At low frequencies $|A_1|$ and $|A_2|$ are of the same order of magnitude; hence, the slope of the phase corresponds to a velocity in between V_1 and V_2.

Figure 6(c) presents the amplitude of the response $\delta\Phi$ due to a line excitation, as a function of distance Δx from the line excitation, at frequency $f = 4$ Hz. From such a function, a relaxation length may be obtained as shown in Fig. 6(c). Repeating this computation for several frequencies, this relaxation length is obtained and presented in Fig. 6(d). It can be seen that the relaxation length is a decreasing function of frequency and this explains Fig. 6(b) and the behavior of the phase in Fig. 6(a).

This analysis suggests that at high frequencies, where attenuation effects are strong, the effect of velocities near the edges of the subassembly predominate and give a slope of the phase different from the slope at lower frequencies, where attenuation effects are less strong and velocities further away from the edges give a measurable contribution, resulting in a smaller slope of the phase.

In the actual case of BWRs, detectors see not only one subassembly but all four subassemblies surrounding the bypass region. Figure 7 presents the cross-spectrum of detectors placed along the middle line of two "channels", each of which has a "turbulent-like" velocity profile, the first one with maximum velocity $V_{max} = 720$ cm/s and the second one with $V_{max} = 640$ cm/s. In both "channels" the peaking factor is 1.428. It can be seen that the phase of the cross-spectrum presents two slopes, similar to the ones observed experimentally.

4. CONCLUSIONS

The present numerical simulation suggests that the double slope of the phase observed in measured cross-spectra at certain BWRs may be the effect of velocity profiles of the void propagation.

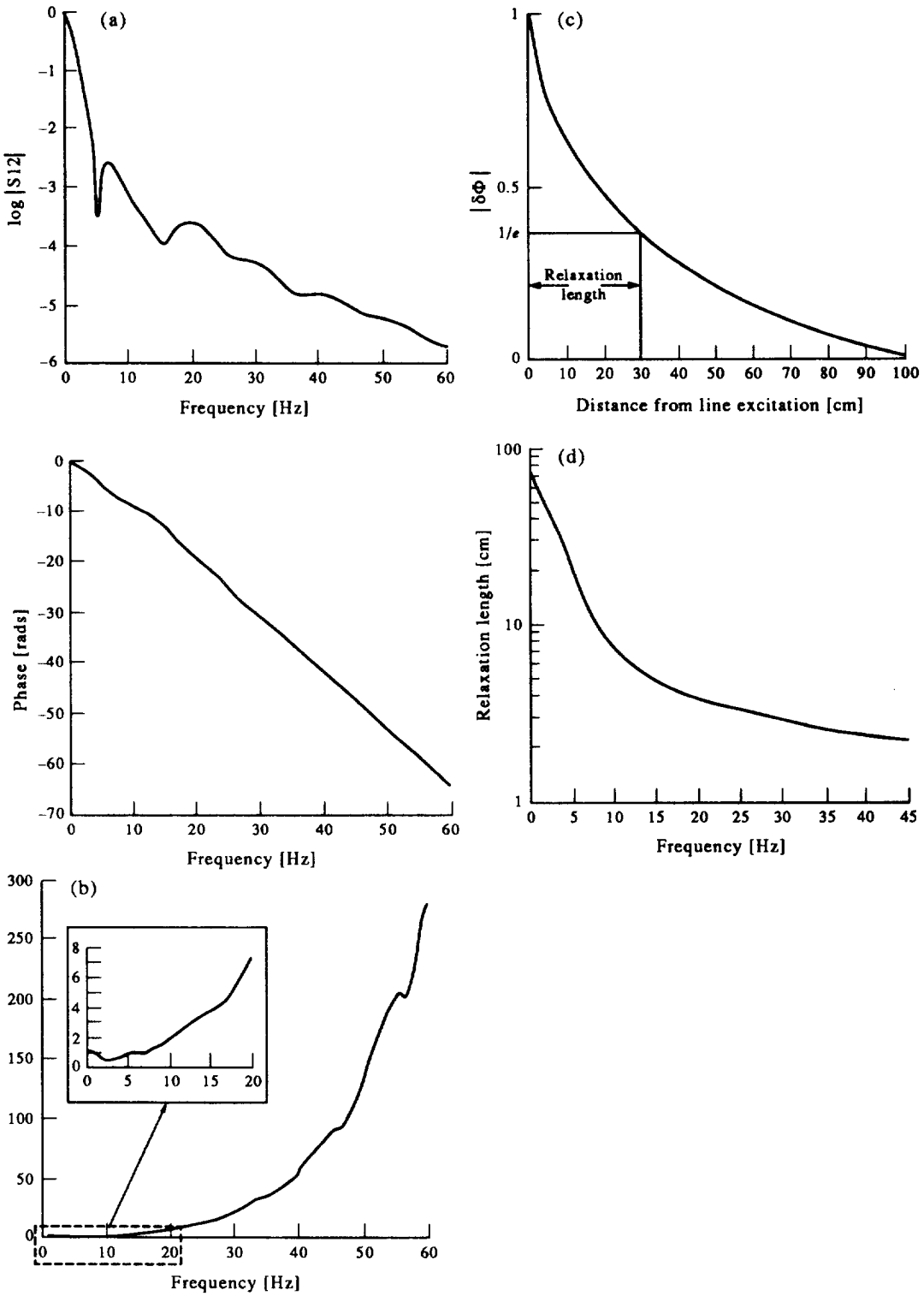

Fig. 6. (a) Neutron cross-spectrum S_{12} between $z_2 = 162$ cm and $z_1 = 72$ cm for two line excitations at different distances from the detectors. (b) The ratio $|A_1|/|A_2|$ as a function of frequency, where $|A_1|, |A_2|$ the responses to the excitations propagating with $V_1 = 504$ cm/s and $V_2 = 720$ cm/s, respectively. (c) Neutron response to a line excitation as a function of distance Δx from the excitation. (d) Relaxation length as a function of frequency.

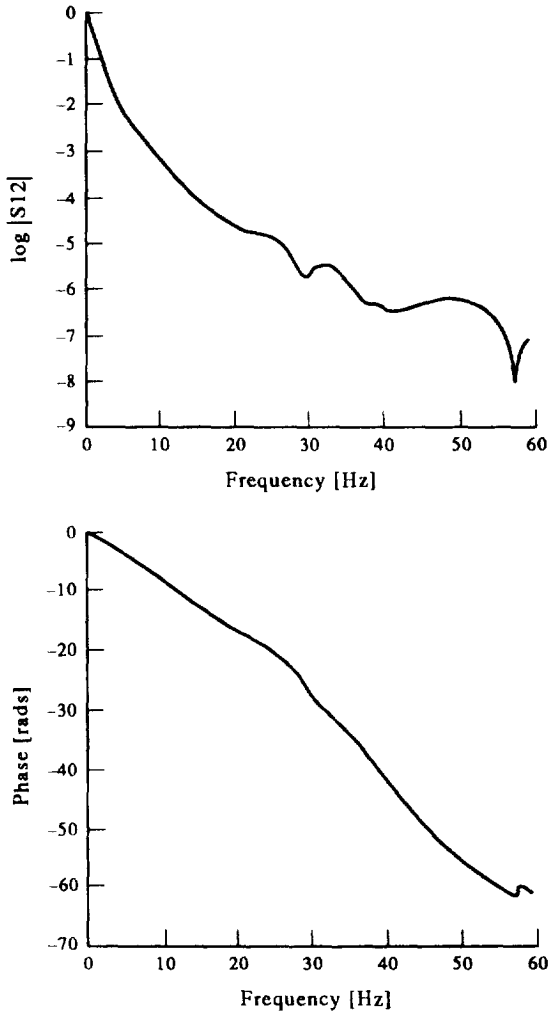

Fig. 7. Neutron cross-spectrum S_{12} between $z_2 = 162$ cm and $z_1 = 72$ cm placed along the middle line of two "channels".

The presence of the profile produces deeps and peaks in the cross-spectra and undulations in the phase which could, in a measurement, be interpreted as different slopes.

Furthermore, the relaxation length of the response is a decreasing function of frequency. Hence, at high frequencies the effect of the velocity at the edge of the subassembly predominates and the slope of the phase corresponds to a velocity near the one at the edge. At low frequencies, where attenuation effects are less strong, subchannels away from the edge give a significant contribution to the neutron response; hence, the slope of the phase at low frequencies is different from the slope at high frequencies.

The velocity profile produces deeps in the magnitude of the cross-spectrum even if global effects are neglected.

REFERENCES

Antonopoulos-Domis M., Kadi S. and Mourtzanos K. (1995) *Ann. Nucl. Energy* **22**, 39.
Behringer K. (1983) *Ann. Nucl. Energy* **10**, 433.
Behringer K. and Crowe R. D. (1981) *Atomkernenergie-Kerntechnik* **38**, 47.

Federico A., Galli C., Parmeggiani C., Ragona R. and Tosi V. (1982) *Prog. Nucl. Energy* **9,** 631.
Kleiss E. B. J., Oosterkamp W. J. and Nissen W. H. M. (1985) *Prog. Nucl. Energy* **15,** 735.
Kosaly G. (1980) *Prog. Nucl. Energy* **5,** 145.
Kosaly G., Kostic L., Miteff, L., Varadi G. and Behringer K. (1977) *Prog. Nucl. Energy* **1,** 99.
Kozma R. (1991) *Proc. 6th Symp. on Nuclear Reactor Surveillance and Diagnostics*, Knoxville, U.S.A., 2, 38.
Luebbesmeyer D. (1983) *Ann. Nucl. Energy* **10,** 421.
Stekelenburg A. J. C. and Van der Hagen T. H. J. J. (1993) *Ann. Nucl. Energy* **20,** 611.